

RESEARCH ARTICLE

RNF144a induces ERK-dependent cell death under oxidative stress via downregulation of vaccinia-related kinase 3

Seung Hyun Han and Kyong-Tai Kim*

ABSTRACT

Vaccinia-related kinase 3 (VRK3) has been reported to be a negative regulator of ERK (ERK1 and ERK2; also known as MAPK3 and MAPK1, respectively) that protects cells from persistent ERK activation and inhibits ERK-dependent apoptosis. Here we report that the E3 ubiquitin–protein ligase RNF144a promotes the degradation of VRK3 via polyubiquitylation and thus affects VRK3-mediated ERK activity. Under oxidative stress, VRK3 migrates from the nucleus to the cytoplasm, which increases its chance of interacting with RNF144a, thereby promoting the degradation of VRK3. Overexpression of RNF144a increases ERK activity via downregulation of VRK3 and promotes ERK-dependent apoptosis. In contrast, depletion of RNF144a increases the protein level of VRK3 and protects cells from excessive ERK activity. These findings suggest that VRK3 protects cells by suppressing oxidative stress-induced ERK, and that RNF144a sensitively regulates this process.

KEY WORDS: ERK signaling, Oxidative stress, Proteasomal degradation, RNF144a, VRK3

INTRODUCTION

ERK signaling, which is one of the most well-known signaling pathway in cells, regulates numerous cellular events, including proliferation, differentiation, apoptosis and cell cycle arrest (Pearson et al., 2001; Zhang and Liu, 2002). Because ERK (here referring to ERK1 and ERK2; also known as MAPK3 and MAPK1, respectively) plays a number of important roles in the cell, ERK activity is regulated by many signaling pathways. Various scaffold proteins have been reported to modulate ERK activity via anchoring protein complexes (Sacks, 2006). There are also several feedback loops in the cell to properly regulate ERK activity (Lake et al., 2016). In addition, several phosphatases dephosphorylate phospho-ERK, to help balance ERK activity in various situations (Kondoh and Nishida, 2007). Even though ERK signaling is known to positively control cell survival, it also regulates anti-proliferative events such as apoptosis and cell cycle arrest. Among these, DNA damaging agents are well known for increasing ERK-dependent apoptosis. In addition, there are several reports that oxidative stress induced by H₂O₂ also increases ERK activity and induces apoptosis (Cagnol and Chambard, 2010; Lu and Xu, 2006). Previous papers showed that H₂O₂-mediated apoptosis induced by activation of ERK is rescued by the ERK inhibitor PD98059 in L929 cells

(Lee et al., 2003). There are other reports that ERK activation by oxidative stress promotes death of osteoblastic cells, which is independent from EGFR signaling (Park et al., 2005). This suggests that the sustained high activity of ERK induced by oxidative stress is a critical factor that increases cell death.

VRK3 is a member of the vaccinia related kinase family, a novel protein whose role is not well understood. VRK3 is known to be expressed ubiquitously in various tissues and is located in the nucleus of most cells (Kang and Kim, 2008). VRK3 was initially reported as a pseudokinase, but was later identified by our group as an active kinase that directly phosphorylates BAF (also known as BANF1) on Ser4 (Park et al., 2015; Scheeff et al., 2009). Phosphorylation of BAF by VRK3 promotes cell proliferation. Recently, we also reported that VRK3-knockout mice exhibit autistic behavior such as reduced social interaction and impairment of learning and memory (Kang et al., 2017). The best-known role of VRK3 is to negatively regulate ERK activity. According to our previous studies, VRK3 plays a role in forming a ternary complex with ERK and VHR (also known as DUSP3) and allows increased action of VHR phosphatase through protein–protein interaction, and the activated VHR promotes ERK dephosphorylation (Kang and Kim, 2006). In addition, phosphorylation of VRK3 by CDK5 under oxidative stress conditions is known to inhibit persistent activation of ERK by increasing VHR phosphatase activity (Song et al., 2016a). Through these pathways, VRK3 protects neuronal cells by inhibiting the persistent activation of ERK. Recently, the role of ERK in neuronal apoptosis has been highlighted (Zhu et al., 2002). It has also been reported that ERK activity is persistently increased in neurodegenerative diseases such as Alzheimer's disease (AD) and Parkinson's disease (PD) (Colucci-D'Amato et al., 2003; Kim and Choi, 2010; Perry et al., 1999). Changes in the localization of HSP70 by VRK3 have been suggested to play a role in inhibiting neuronal cell death in the brains of AD and PD patients (Song et al., 2016b). Although VRK3 is one of the key molecules that regulate the cell cycle and ERK activity, as described above, the mechanism of how VRK3 itself is regulated is not known at all.

RNF144a is a member of the RNF144 family of E3 protein–ubiquitin ligases (E3 ligases), which have an RBR domain at the N-terminus (Smit and Sixma, 2014; Spratt et al., 2014). Previous reports have shown that RNF144a regulates the stability of DNA-PK to increase apoptosis in DNA damage situations and decrease cellular sensitivity to the PARP1 inhibitor by ubiquitylating PARP1 (Ho et al., 2014; Zhang et al., 2017). In addition, RNF144a is known to trigger a sustained EGF signal by inducing polyubiquitylation of EGFR (Ho and Lin, 2018). It has been reported that RNF144a promotes cell death when DNA damage occurs, but the function of RNF144a under oxidative stress is still unknown.

In this study, we found that localization of VRK3 was altered by oxidative stress. RNF144a promotes polyubiquitylation of VRK3 and the degradation of VRK3 in the cytosol. Degradation of VRK3 by RNF144a enables sustained activation of ERK, making cells

Division of Integrative Biosciences and Biotechnology, Pohang University of Science and Technology, Pohang 37673, Republic of Korea.

*Author for correspondence (ktk@postech.ac.kr)

 S.H.H., 0000-0002-0909-3659; K.-T.K., 0000-0001-7292-2627

Handling Editor: Michael Way

Received 7 April 2020; Accepted 17 September 2020

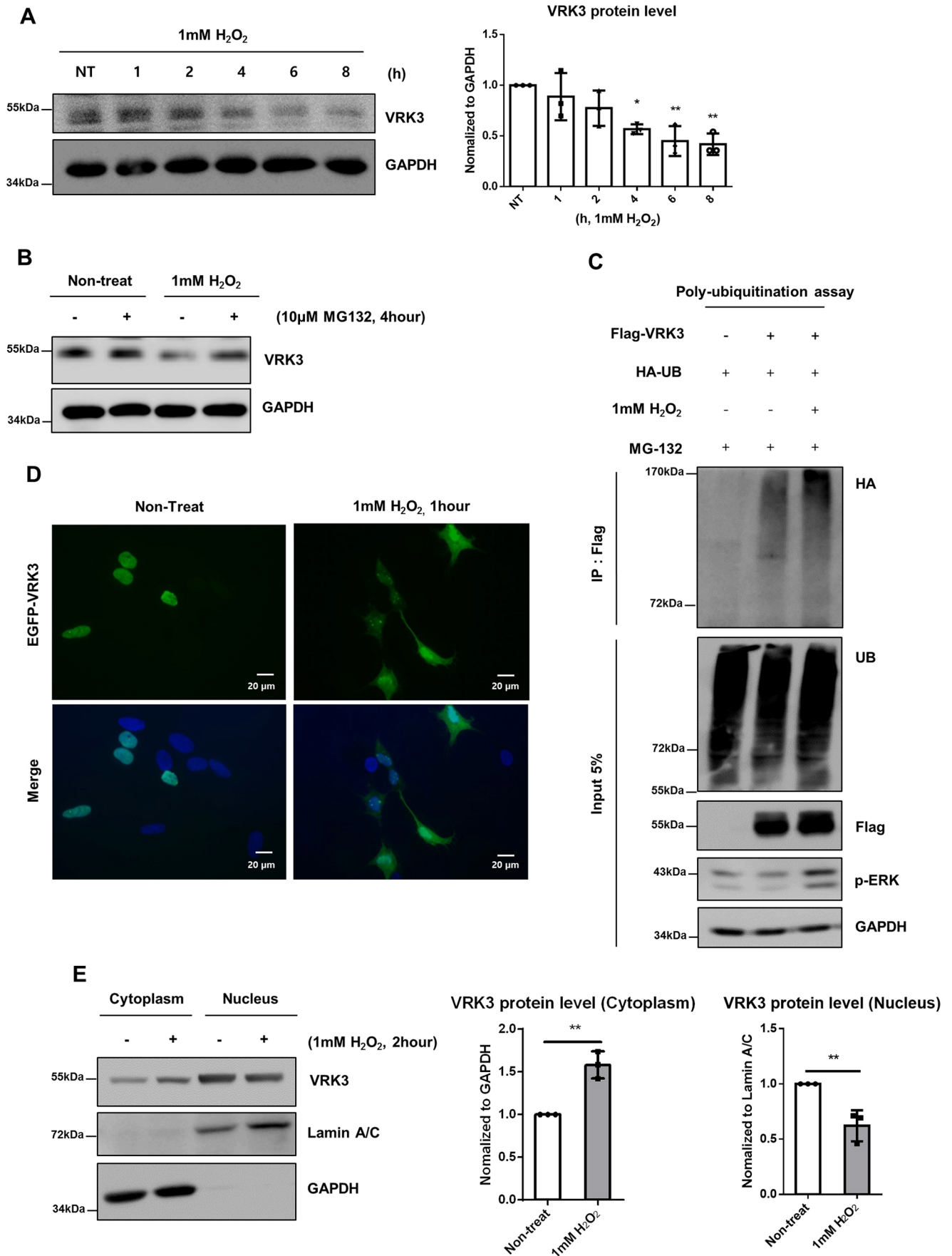


Fig. 1. See next page for legend.

Fig. 1. Change in localization and protein level of VRK3 under oxidative stress. (A) VRK3 protein level decreases under oxidative stress. U2OS cells were treated with 1 mM H₂O₂ for 1, 2, 4, 6 and 8 h. Cell lysates were analyzed by immunoblotting. VRK3 levels were normalized to GAPDH. Values represent mean±s.d. (*n*=3 independent experiments). **P*<0.05; ***P*<0.01 (Tukey's multiple comparison test). (B) VRK3 degradation is UPS dependent. U2OS cells were treated with 10 μM MG132 for 4 h and subsequently treated with 1 mM H₂O₂ for 1 h. Cell lysates were analyzed by immunoblotting. Samples without H₂O₂ treatment are also shown (Non-treat). GAPDH is shown as a loading control. Data are representative of three independent experiments. (C) VRK3 polyubiquitylation increases under oxidative stress. HEK293A cells were transfected with the indicated vectors and treated with 10 μM MG132 for 4 h. The effects of oxidative stress were assayed following 1 mM H₂O₂ treatment. Cell lysates were immunoprecipitated (IP) with anti-Flag antibody, and VRK3 polyubiquitylation was analyzed by immunoblotting. GAPDH is shown as a loading control. p-ERK, phosphorylated ERK; UB, ubiquitin. Data are representative of two independent experiments. (D) Localization of EGFP–VRK3 in response to H₂O₂ was observed using fluorescence microscopy. Nuclei in merge images are labeled by Hoechst 33342 (blue). Data are representative of three independent experiments. (E) H₂O₂ triggers the translocation of VRK3 from the nucleus to the cytoplasm. U2OS cells were treated with 1 mM H₂O₂ for 2 h, and cell lysates were analyzed in nucleoplasmic and cytoplasmic fractions. Values represent mean±s.d. (*n*=3 independent experiments). ***P*<0.01 (two-tailed unpaired *t*-test).

more sensitive to oxidative stress. In contrast, the increase of VRK3 due to the depletion of RNF144a downregulates ERK activity and decreases ERK-dependent cell death.

Taken together, our observations indicate that RNF144a reduces the stability of VRK3 and increases ERK-mediated cell death under oxidative stress.

RESULTS

Protein level and localization of VRK3 change under oxidative stress

We first tried to determine how the characteristics of VRK3 change under oxidative stress in the U2OS cell line. Although VRK3 is known to be a molecule that regulates ERK signaling in response to H₂O₂, it remains largely unknown how VRK3 itself is regulated. U2OS cells have been widely studied under oxidative stress situations (Fu et al., 2017; Peugeot et al., 2014; Xu et al., 2014). Also, the role of RNF144a, which regulates the stability of DNA-PK during DNA damage stress, has been identified in U2OS cells (Redza-Dutoridoir and Averill-Bates, 2016). Therefore, we thought it would be suitable to study the regulation of VRK3 and the role of RNF144a under oxidative stress using U2OS cells.

We found that the protein expression level of VRK3 decreased in response to H₂O₂ treatment, which is known to induce oxidative stress (Fig. 1A). We examined whether H₂O₂ influences not only VRK3 but also the levels of other VRK family members, VRK1 and VRK2. The level of VRK2 was gradually decreased by H₂O₂ exposure, but the level of VRK1 did not change significantly (Fig. S1C). Therefore, protein degradation under oxidative stress was specific to VRK3 and VRK2, but not VRK1. We also observed this pattern in HeLa cells and HMO6 cells (Fig. S1A,B). To confirm whether the decrease in VRK3 level during oxidative stress was due to degradation by the proteasome, we treated cells with MG132, which is known as a proteasome inhibitor. We found that VRK3 reduction by H₂O₂ treatment was rescued by the treatment with MG132 (Fig. 1B). The polyubiquitylation of VRK3 was increased under oxidative stress, indicating that the degradation of VRK3 was caused by the ubiquitin–proteasome system (UPS) (Fig. 1C). Because VRK3 has a nuclear localization signal (NLS) and is known to be located in the nucleus, we examined the localization of VRK3 under oxidative stress to determine whether the degradation of VRK3 occurs in the nucleus or

cytoplasm (Nichols and Traktman, 2004). Interestingly, EGFP–VRK3 was translocated from nucleus to cytoplasm in response to H₂O₂ (Fig. 1D). To confirm the translocation of VRK3, we analyzed nucleoplasmic and cytoplasmic VRK3 in response to H₂O₂. In the absence of oxidative stress, most VRK3 remained in the nucleus, but under oxidative stress, VRK3 in the nucleus was translocated to the cytoplasm (Fig. 1E). We found that the translocation of VRK3 is an important event in the VRK3 degradation, because treatment with the nuclear export inhibitor Leptomycin B inhibited H₂O₂-mediated VRK3 degradation (Fig. S1D). Taken together, these results indicate that H₂O₂ induces the degradation of VRK3 via the UPS and the translocation of VRK3 from the nucleus to the cytoplasm.

VRK3 binds to RNF144a

We speculated that there might be an E3 ligase that accelerates the degradation of VRK3 under oxidative stress. However, an E3 ligase that regulates VRK3 stability has not been reported yet. In another study, we investigated the relationship between VRK3 and PARP1. There, we observed that RNF144a, which is known as an E3 ligase of PARP1, also reduces the amount of VRK3 (S.H.H. and K.-T.K., unpublished). Therefore, we tried to determine whether RNF144a is an E3 ligase that also promotes VRK3 degradation. First, we performed immunoprecipitation to observe whether VRK3 and RNF144a bind to each other. We observed that endogenous RNF144a was immunoprecipitated by an anti-VRK3 antibody (Fig. 2A). We also overexpressed Flag-tagged VRK3 or Flag-tagged RNF144a in HEK293a cells and immunoprecipitated with an anti-Flag antibody. We found that Flag–VRK3 interacted with endogenous RNF144a, and vice versa (Fig. S2A,B). We performed a GST pull-down assay to determine whether VRK3 directly binds to RNF144a. We found that purified recombinant GST–RNF144a bound to His–VRK3, and the result was confirmed by a reciprocal GST pull-down assay (Fig. 2B; Fig. S2C). Next, we performed a GST pull-down assay using fragments of recombinant VRK3 to determine which VRK3 domain binds to RNF144a. We found that purified full-length GST–VRK3 and fragmentary GST–VRK3-F1 (amino acids 1–165) pulled down His–RNF144a (Fig. 2C,D). Taken together, we observed that the N-terminal of VRK3 physically interacts with RNF144a.

RNF144a promotes polyubiquitylation of VRK3

Because RNF144a is known as an E3 ligase, we tested whether RNF144a regulates the stability of VRK3 via the UPS. Interestingly, although the protein level of VRK3 was significantly decreased by overexpression of RNF144a, there was no difference in the mRNA level of *VRK3* (Fig. 3A,B). RNF144a overexpression also decreased the level of VRK3 in HeLa cells (Fig. S3B). In order to examine the effect of RNF144a knockdown on VRK3, we transfected small interfering RNA (siRNA) targeting RNF144a into U2OS cells. Knockdown of RNF144a increased the protein level of VRK3 but did not affect the mRNA level of *VRK3* (Fig. 3C,D). From this observation, we could see that RNF144a is a critical protein that regulates the level of VRK3, and that RNF144a does not regulate gene expression of VRK3 but regulates the protein level of VRK3 in some other way. To exclude off-target effects of siRNA treatment, we used two different siRNAs (sequences are listed in Table S1). Both siRNAs with different sequences induced an increase in VRK3 protein level, but the effect was more pronounced with siRNF144a#2 (Fig. S3A). Therefore, we used siRNF144a#2 for subsequent experiments.

We next tested whether RNF144a modulates VRK3 stability. To date, no E3 ligase has been reported to modulate the stability of

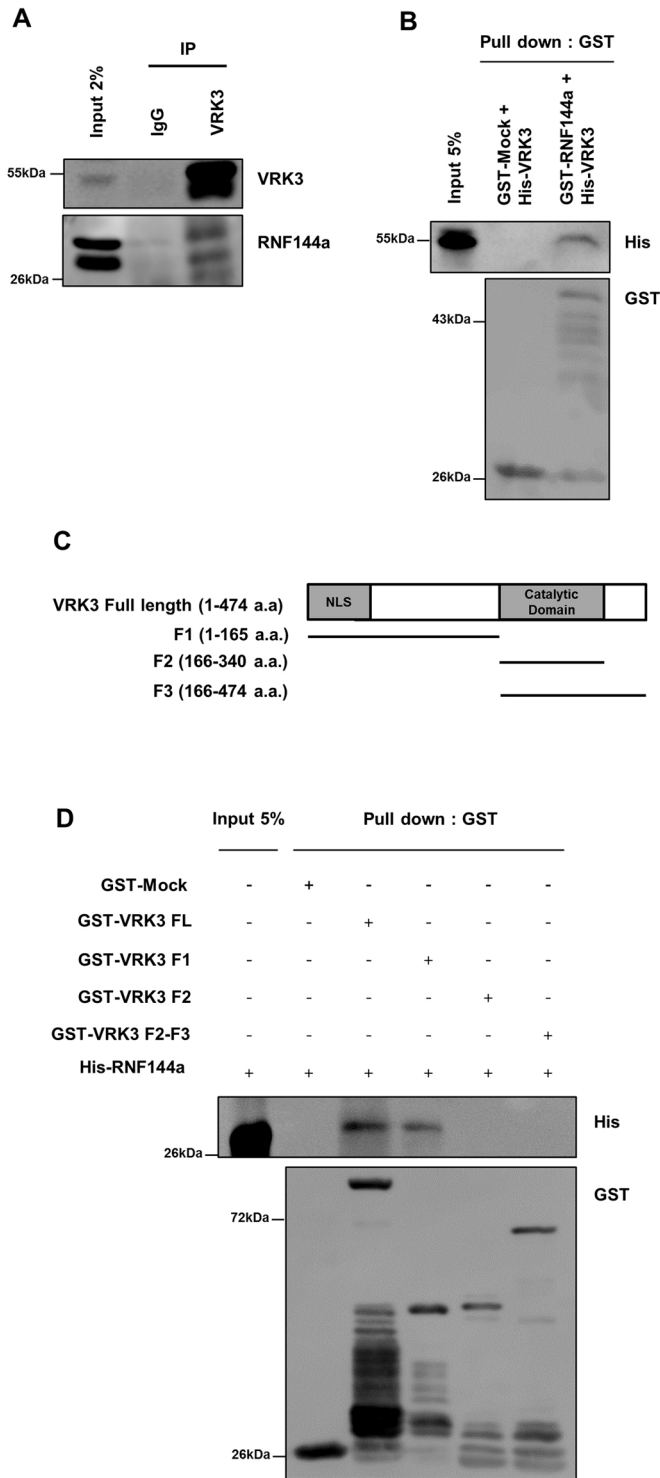


Fig. 2. VRK3 directly interacts with RNF144a via the F1 domain. (A) VRK3 binds to RNF144a. HEK293A cell lysates (1 mg) were immunoprecipitated (IP) with normal IgG or anti-VRK3 antibody. Immunoprecipitates were analyzed by immunoblotting. Data are representative of three independent experiments. (B) VRK3 directly interacts with RNF144a. GST pull-down assays were performed using the indicated recombinant proteins (GST-Mock, GST only control). Data are representative of two independent experiments. (C,D) RNF144a interacts with the F1 domain of VRK3. Recombinant His-RNF144a was mixed with GST alone or GST-VRK3 fragments, followed by GST pull-down. Samples were analyzed by immunoblotting (a.a., amino acids; FL, full length). Data are representative of two independent experiments.

VRK3. Interestingly, reduced VRK3 protein level due to overexpression of RNF144a was rescued by MG132 treatment (Fig. 3E). To additionally confirm whether RNF144a regulates the stability of VRK3, we performed a cycloheximide chase assay. Cycloheximide, which is a translation elongation inhibitor, is widely used to determine protein half-life. We repeatedly confirmed that RNF144a promotes the degradation of VRK3 by observing dramatic reduction in the half-life of HA-VRK3 upon overexpression of RNF144a (Fig. 3F). We next performed an ubiquitylation assay to confirm that RNF144a-mediated downregulation of VRK3 was caused by elevated polyubiquitylation. We found that overexpression of RNF144a dramatically increased the polyubiquitylation of VRK3 and that depletion of RNF144a decreased polyubiquitylation of VRK3 (Fig. 3G,H). In order to exclude the potential off-target effect of siRNA treatment, an independent set of polyubiquitylation assays was performed using siRNF144a#1 (Fig. S3C). We checked which domain of RING1 and RING2 within RNF144a was required for VRK3 ubiquitylation. It has been reported that DNA-PK ubiquitylation requires both RING1 and RING2 domain within RNF144a, and in the case of PARP1 ubiquitylation, the RING2 domain of RNF144a is required (Ho et al., 2014; Zhang et al., 2017). Overexpression of wild-type RNF144a induced an increase in VRK3 ubiquitylation but overexpression of RNF144a C20A/C23A and C198A mutants, which lack activity of the RING1 and RING2 domain, respectively, did not (Fig. S3D,E). Through this, it was confirmed that both the RING1 and RING2 domains within RNF144a are important for ubiquitylation of VRK3. Taken together, our observations indicate that RNF144a is a novel E3 ligase targeting VRK3 that promotes degradation of VRK3 through the UPS.

Degradation of VRK3 by RNF144a increases under oxidative stress

Previously, localization of RNF144a has been reported to be mainly distributed in the endosome and plasma membrane. According to a previous report, RNF144a might promote the degradation of its target protein in the cytoplasm (Ho et al., 2014). The results presented in Fig. 1 show that VRK3 localization changed under oxidative stress conditions. Therefore, we examined whether oxidative stress increased the chance of binding between VRK3 and RNF144a. First, we observed the localization of VRK3 and RNF144a under oxidative stress using immunocytochemistry. Because the antibodies that detect the localization of the endogenous RNF144a are limited, we overexpressed Flag-tagged RNF144a and detected the localization of RNF144a using an anti-Flag antibody. In the absence of oxidative stress, VRK3 was predominantly present in the nucleus and RNF144a was mainly present in cytoplasm. However, under oxidative stress, yellow signals were observed in the cytoplasmic space, indicating that H_2O_2 treatment increases the probability of physical interaction between VRK3 and RNF144a in the cytoplasm (Fig. 4A). To determine whether overexpression of RNF144a promotes the degradation of cytoplasmic VRK3, we performed subcellular fractionation. Overexpression of RNF144a did not affect the level of VRK3 in the nucleus, but significantly decreased the level of VRK3 in the cytoplasm (Fig. S4A). This suggests that RNF144a-mediated degradation of VRK3 is promoted in the cytoplasm. Next, we examined whether overexpression of RNF144a promotes the degradation of VRK3 upon H_2O_2 treatment. A greater reduction in VRK3 level was observed after H_2O_2 treatment in the presence of RNF144a overexpression, compared to the reduction when RNF144a alone was overexpressed (Fig. 4B). Conversely, VRK3, which was degraded under stress, was not

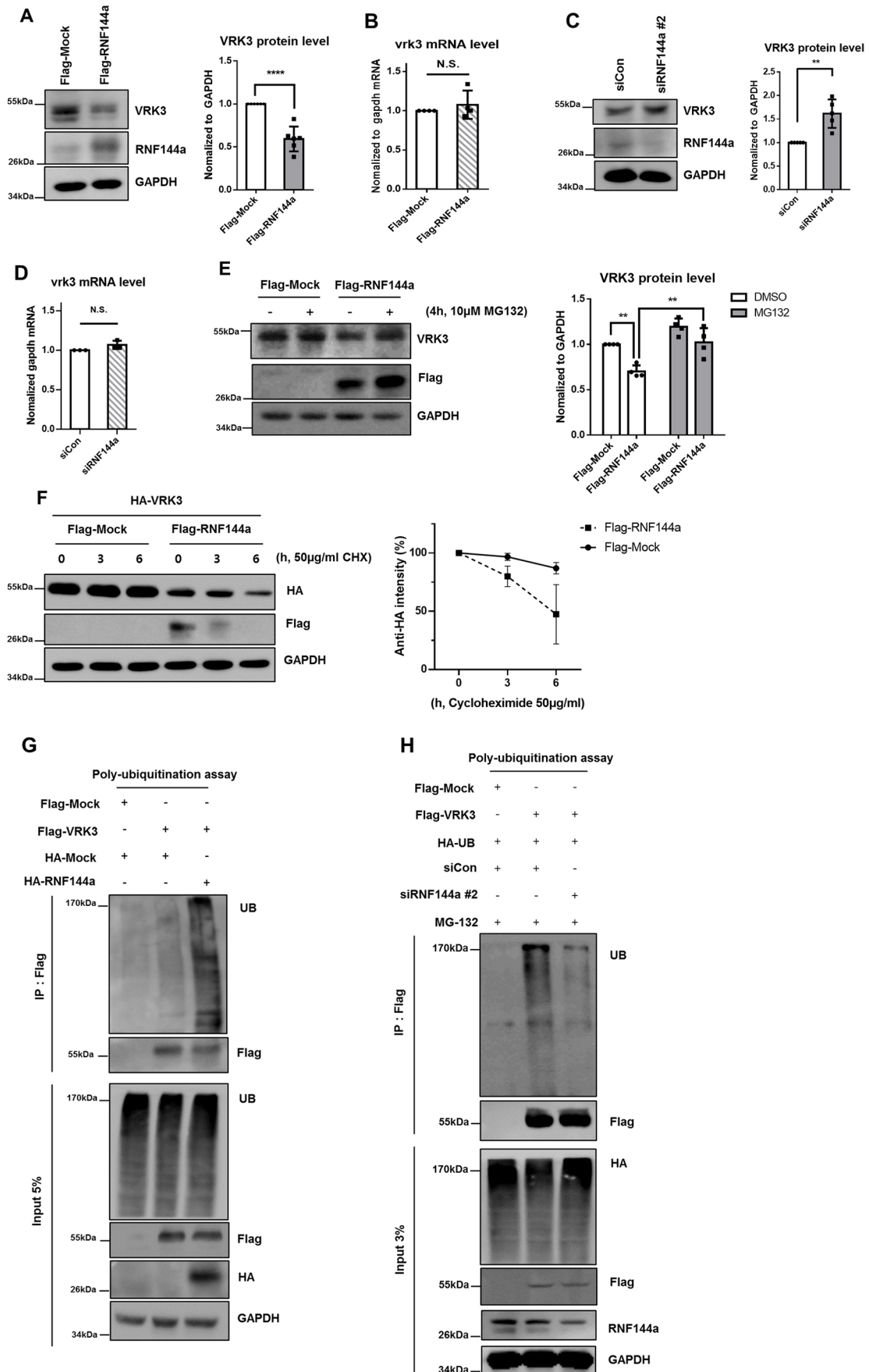


Fig. 3. See next page for legend.

Fig. 3. RNF144a regulates the stability of VRK3. (A) Overexpression of RNF144a leads to a decrease in the protein level of VRK3. U2OS cells were transfected with Flag-RNF144a or Flag tag alone (Flag-Mock). VRK3 levels were normalized to GAPDH. Values represent mean \pm s.d. ($n=6$ independent experiments). **** $P<0.0001$ (two-tailed unpaired t -test). (B) Overexpression of RNF144a does not affect the gene expression of VRK3. VRK3 mRNA was examined by RT-qPCR and normalized to GAPDH mRNA levels. Values represent mean \pm s.d. ($n=4$ independent experiments). N.S., not significant (two-tailed unpaired t -test). (C) Knockdown of RNF144a by siRNA treatment leads to increase in the protein level of VRK3. VRK3 levels were normalized to GAPDH. U2OS cells were transfected with siRNF144a#2 or a control non-targeting siRNA (siCon). Values represent mean \pm s.d. ($n=5$ independent experiments). ** $P<0.01$ (two-tailed unpaired t -test). (D) Knockdown of RNF144a does not affect the gene expression of VRK3. VRK3 mRNA was examined by RT-qPCR and normalized to GAPDH mRNA levels. Values represent mean \pm s.d. ($n=3$ independent experiments). N.S., not significant (two-tailed unpaired t -test). (E) RNF144a promotes degradation of VRK3 via the UPS. U2OS cells were transfected with the indicated vectors, and cells in each group were treated with DMSO (–) or 10 μ M MG132 (+) for 4 h. Cell lysates were analyzed by immunoblotting. VRK3 levels were normalized to GAPDH. Values represent mean \pm s.d. ($n=4$ independent experiments). ** $P<0.01$ (Tukey's multiple comparison test). (F) Overexpression of RNF144a decreases the half-life of HA-VRK3. U2OS cells were transfected with the indicated vectors. Cells were treated with 50 μ g/ml cycloheximide and harvested at the indicated time points. Cell lysates were analyzed by immunoblotting. Quantification of HA-VRK3 protein level was normalized to GAPDH. Values represent mean \pm s.d. ($n=3$ independent experiments). (G,H) RNF144a promotes VRK3 polyubiquitylation. (G) HEK293A cells were transfected with the indicated vectors. The cell lysates were immunoprecipitated (IP) with anti-Flag antibody, and VRK3 polyubiquitylation was analyzed by immunoblotting. (H) HEK293A cells were transfected with the indicated siRNAs (siRNF144a#2 or siCon) and vectors. Transfected cells were treated with 10 μ M MG132 for 4 h. The cell lysates were immunoprecipitated with anti-Flag antibody, and VRK3 polyubiquitylation was analyzed by immunoblotting. UB, ubiquitin. Data in G and H are representative of three independent experiments.

significantly decreased following H₂O₂ treatment when RNF144a was depleted (Fig. 4C). An independent experiment was performed using siRNF144a#1 (Fig. S4B). This suggests that RNF144a has a crucial role in controlling the degradation of VRK3 under oxidative stress. We checked whether the level of RNF144a also changes under oxidative stress. Previous studies have reported that the expression of RNF144a increases in a p53-dependent manner in DNA damage situations (Ho et al., 2014). In our case, we observed the tendency of a slight increase in the level of RNF144a under oxidative stress through five independent experiments, but the increase was not statistically significant (Fig. S4C). These results show that the increase in RNF144a induced by the stress might contribute to VRK3 degradation. Additionally, we found that polyubiquitylation of VRK3 was greatly increased upon overexpression of RNF144a in the presence of H₂O₂ treatment (Fig. 4D). This means that under oxidative stress, RNF144a increases polyubiquitylation of VRK3 followed by proteasome-mediated degradation. From the data above, we can deduce that translocation of VRK3 from the nucleus to the cytoplasm by oxidative stress induces increased interaction between VRK3 and RNF144a, which promotes UPS-mediated protein degradation of VRK3.

Degradation of VRK3 by RNF144a regulates ERK signaling independently of EGFR signaling

Our group has previously reported that VRK3 is a negative regulator of ERK (Lake et al., 2016). Therefore, we hypothesized that the degradation of VRK3 induced by oxidative stress would affect ERK activity. To determine whether reduced VRK3 increases ERK phosphorylation as previously reported, we compared the ERK activity in VRK3-knockdown cells to the activity in control cells. As

expected, ERK activity was increased when the protein level of VRK3 was decreased (Fig. 5A). We repeatedly confirmed this tendency using two independent shRNAs targeting VRK3 (Fig. S5A,B and Table S1). We next examined whether the reduction of VRK3 by overexpression of RNF144a increased ERK activity. As we increased the expression of RNF144a, the level of VRK3 decreased correspondingly and the phosphorylation of ERK was increased (Fig. 5B). Because ERK phosphorylation increases under oxidative stress (Cagnol and Chambard, 2010), we examined whether an increase in ERK phosphorylation due to overexpression of RNF144a was affected by H₂O₂ treatment. Overexpression of Flag-RNF144a promoted degradation of VRK3, and phosphorylation of ERK was increased compared to that in the control (Fig. 5C). In contrast, H₂O₂-induced ERK phosphorylation was decreased in RNF144a-knockdown cells compared to that observed for control cells (Fig. 5D). Previously, it was reported that RNF144a regulates the activity of ERK through EGFR signaling (Ho and Lin, 2018). Therefore, we examined whether changes in ERK phosphorylation by overexpression of RNF144a under oxidative stress were independent of EGFR signaling. To confirm the activity of ERK independent of EGFR, we treated U2OS cells with AG1478, which is an EGFR inhibitor. As previously reported, when RNF144a was overexpressed, the phosphorylation of EGFR and ERK was increased. However, the phosphorylation of ERK was still increased even under AG1478 treatment (Fig. 5E). This suggests that there may be another factor that increases ERK phosphorylation independently of EGFR signaling. Because VRK3 protein level was markedly decreased when RNF144a was overexpressed, we speculated that the increase in ERK phosphorylation might be due to a reduction of VRK3. EGFR signaling is well known to simultaneously increase phosphorylation of AKT as well as phosphorylation of ERK (El-Rayes and LoRusso, 2004). Therefore, we examined the relationship between RNF144a and EGFR signaling by observing phosphorylation of both ERK and AKT. Interestingly, the amount of AKT phosphorylation induced by oxidative stress was similar regardless of the overexpression of RNF144a, whereas the phosphorylation of ERK was increased even more when RNF144a was overexpressed compared to the control condition (Fig. 5F). This suggests that there is an independent mechanism, which increases the phosphorylation of ERK only rather than increasing phosphorylation of both ERK and AKT. To determine whether the increase in ERK activity upon overexpression of RNF144a was dependent on VRK3, we re-introduced VRK3 into U2OS cells. We observed that overexpression of VRK3 decreased ERK activity, even though the RNF144a level was high. As a result, we confirmed that VRK3, which is regulated by RNF144a, is an important factor in the regulation of ERK activity (Fig. 5G). Taken together, we found that RNF144a increases the activity of ERK via downregulation of VRK3 in response to H₂O₂, which is independent of EGFR signaling.

RNF144a promotes ERK-mediated apoptosis via downregulation of VRK3 under oxidative stress

According to our previous reports, phosphorylation of VRK3 by CDK5 under oxidative stress increases the activity of VHR phosphatase and plays a protective role against oxidative stress. We found that depletion of VRK3 makes cells more sensitive to oxidative stress (Song et al., 2016a). Therefore, we examined how the reduction of VRK3 protein level by overexpression of RNF144a affects cell viability under oxidative stress. Reduction of VRK3 by overexpression of RNF144a increased the levels of cleaved caspase 3, which is a marker for apoptosis (Fig. 6A). To confirm whether the overexpression of RNF144a makes cells sensitive to oxidative stress, we conducted an

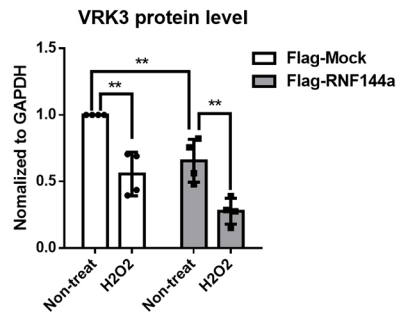
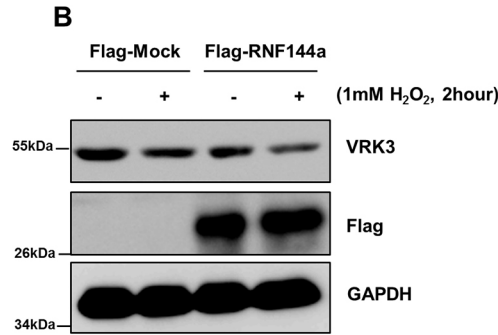
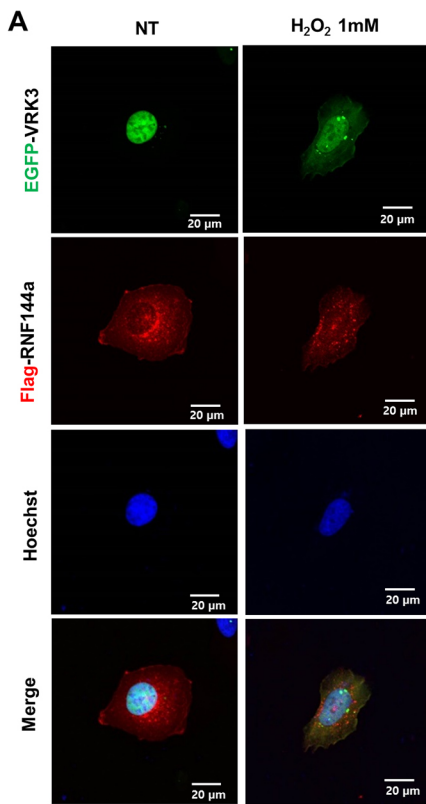
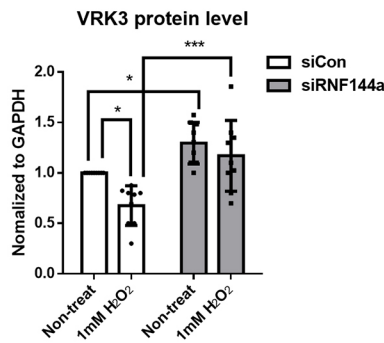
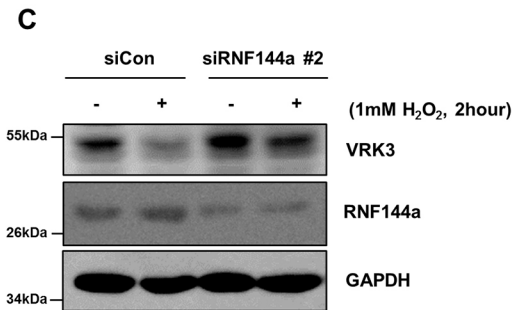


Fig. 4. RNF144a promotes the degradation of VRK3 under oxidative stress. (A) Localization of VRK3 and RNF144a in response to H₂O₂. U2OS cells were transfected with EGFP-VRK3 and Flag-RNF144a. Localization of EGFP-VRK3 and Flag-RNF144a in response to H₂O₂ was observed by confocal microscopy (Non-treat, no H₂O₂ treatment control). Hoechst staining (blue) indicates nuclei. Data are representative of three independent experiments.

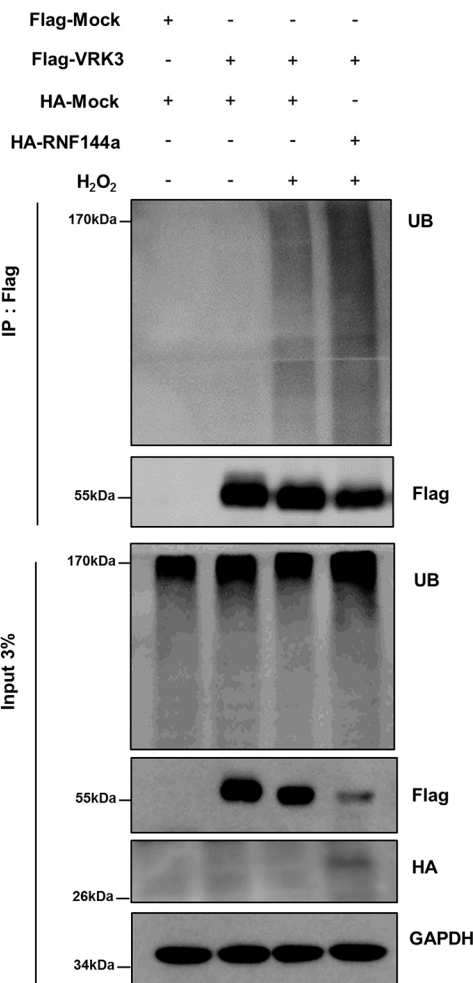
(B) RNF144a promotes the degradation of VRK3 in response to H₂O₂. U2OS cells were transfected with Flag-RNF144a or control vector (Flag-Mock). Cells were treated with 1 mM H₂O₂ or vehicle for 2 h. The cell lysates were analyzed by immunoblotting. VRK3 levels were normalized to GAPDH. Values represent mean±s.d. (*n*=4 independent experiments). ***P*<0.01 (Tukey's multiple comparison test).

(C) RNF144a is crucial for H₂O₂-mediated VRK3 degradation. U2OS cells were transfected with siRNF144a#2 or non-targeting control siRNA (siCon). Cells were treated with 1 mM H₂O₂ or vehicle for 2 h. The cell lysates were analyzed by immunoblotting. VRK3 levels were normalized to GAPDH. Values represent mean±s.d. (*n*=9 independent experiments). **P*<0.05; ****P*<0.001 (Tukey's multiple comparison test).

(D) RNF144a promotes proteasome-mediated VRK3 degradation in response to H₂O₂. HEK293A cells were transfected with the indicated constructs. Cells were treated with 1 mM H₂O₂ for 1 h. Cell lysates were immunoprecipitated (IP) with anti-Flag antibody and VRK3 polyubiquitylation was analyzed by immunoblotting. Data are representative of three independent experiments.



D Poly-ubiquitination assay



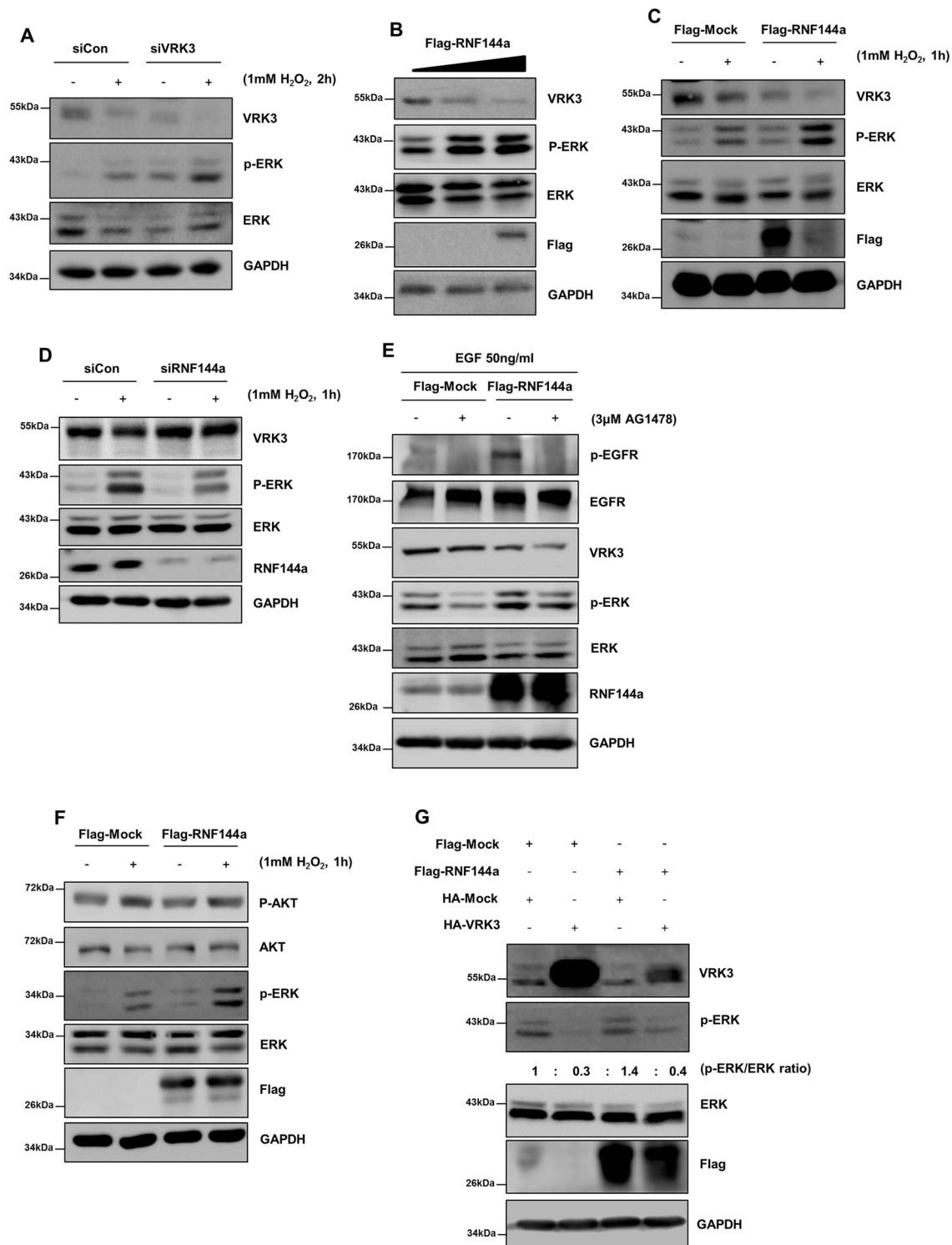


Fig. 5. RNF144a increases ERK activity independently of EGFR signaling. (A) VRK3 is a negative regulator of the ERK pathway. U2OS cells were transfected with either siVRK3 or a control siRNA (siCon). Cells were treated with 1 mM H₂O₂ for 2 h. The cell lysates were analyzed by immunoblotting. p-ERK, phosphorylated ERK. (B) RNF144a increases the activity of ERK, as indicated by levels of p-ERK. U2OS cells were transfected with Flag-RNF144a at different concentrations. Cell lysates were analyzed by immunoblotting. (C) RNF144a increases the activity of ERK in response to H₂O₂, as indicated by levels of p-ERK. U2OS cells were transfected with Flag-RNF144a or control vector (Flag-Mock) and cells were treated with 1 mM H₂O₂ for 1 h. Cell lysates were analyzed by immunoblotting. (D) Knockdown of RNF144a (siRNF144a) decreases the activity of ERK in response to H₂O₂, as indicated by levels of p-ERK. Cell lysates were analyzed by immunoblotting. (E) RNF144a-mediated increase in ERK activity is EGFR independent. U2OS cells were transfected with Flag-RNF144a or control vector and treated with 3 μM AG1478 for 30 min, followed by stimulation with 50 ng/ml EGF for 15 min. Cell lysates were analyzed by immunoblotting. (F) U2OS cells were transfected with Flag-RNF144a or control vector and treated with 1 mM H₂O₂ for 1 h. Cell lysates were analyzed by immunoblotting. P-AKT, phosphorylated AKT. (G) Re-introduction of VRK3 decreases the ERK activity induced by overexpression of RNF144a. U2OS cells were transfected with the indicated vectors and cells were treated with 1 mM H₂O₂ for 1 h. Cell lysates were analyzed by immunoblotting. The ratio of p-ERK to ERK signal for the representative blot is indicated. Data in A–G are representative of at least three independent experiments.

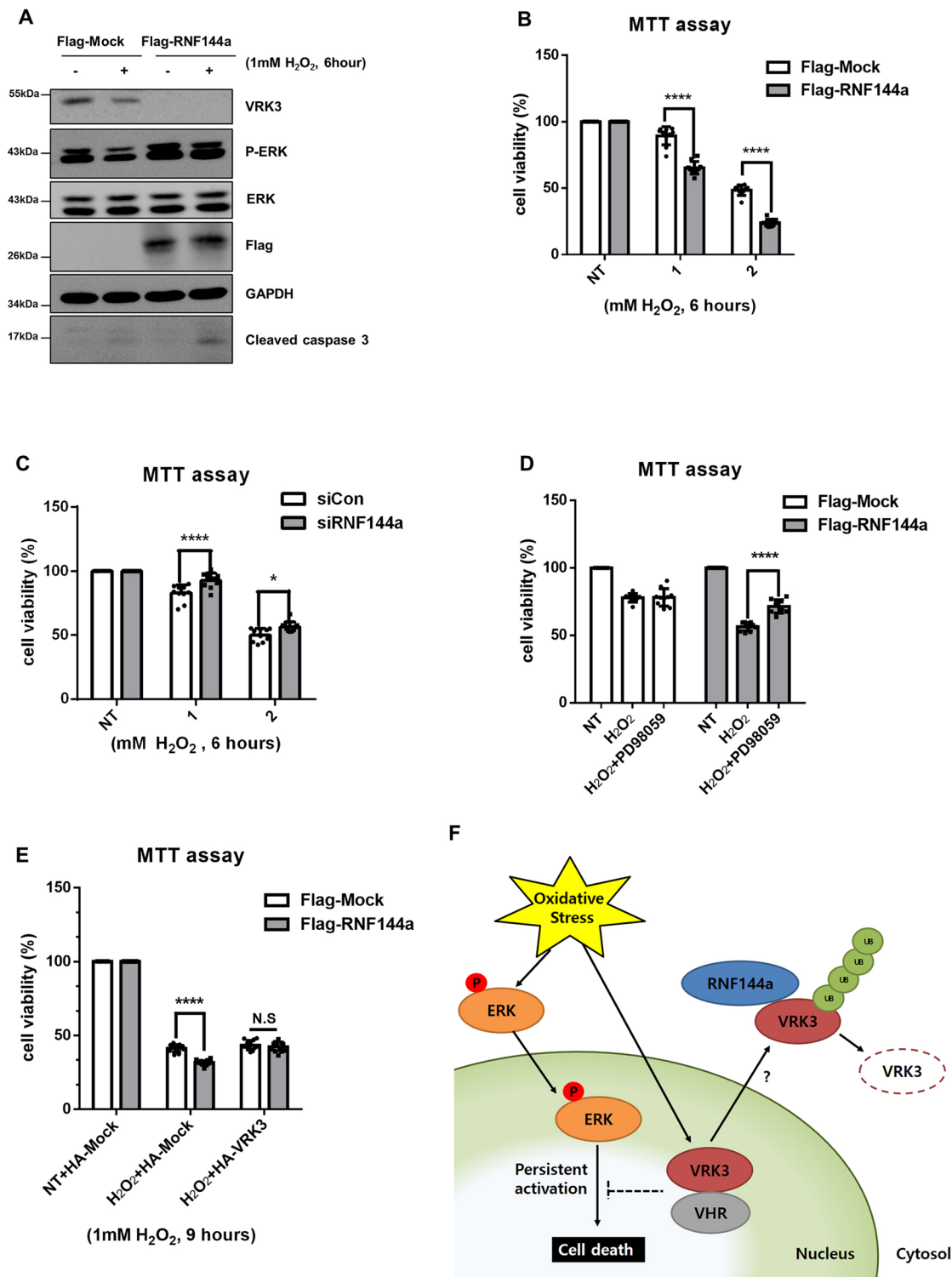


Fig. 6. RNF144a induces ERK-dependent apoptosis under oxidative stress. (A) RNF144a increases sensitivity of U2OS cells to H₂O₂. U2OS cells were transfected with Flag-RNF144a or control vector (Flag-Mock). Cells were treated with 1 mM H₂O₂ for 6 h. Cell lysates were analyzed by immunoblotting (P-ERK, phosphorylated ERK). Data are representative of three independent experiments. (B, C) U2OS cells were transfected with Flag-RNF144a or control vector, or siRNF144a#2 or control siRNA (siCon). Cells were treated with H₂O₂ [0 (NT), 1 or 2 mM] for 6 h, and cell viability was detected using 3-(4,5-dimethylthiazol-2-yl)-2,5-diphenyltetrazolium bromide (MTT). *n*=10. **P*<0.05; *****P*<0.0001 (Tukey's multiple comparison test). (D) RNF144a increases ERK-dependent apoptosis. U2OS cells were transfected with Flag-RNF144a or control vector. Cells were either treated with 1 mM H₂O₂ for 6 h or left untreated (NT), followed by inhibition of ERK activity with 50 μM PD98059 or treatment with vehicle (DMSO). Cell viability was detected using MTT. *n*=10. *****P*<0.0001 (Tukey's multiple comparison test). (E) Re-introduction of VRK3 rescues the RNF144a-mediated apoptosis in response to H₂O₂. U2OS cells were transfected with the indicated vectors and treated with 1 mM H₂O₂ for 9 h. Cell viability was detected using MTT. *n*=10. N.S., not significant; *****P*<0.0001 (Tukey's multiple comparison test). (F) Proposed diagram for the RNF144a-mediated cell death via VRK3 downregulation under oxidative stress. Under oxidative stress, VRK3 is translocated from the nucleus to the cytoplasm, and RNF144a promotes the degradation of cytoplasmic VRK3 via the UPS. Oxidative-stress-mediated degradation of VRK3 leads to persistent ERK activation and promotes apoptosis.

MTT assay. Overexpression of RNF144a promoted more cell death under oxidative stress (Fig. 6B). In contrast, transient transfection with siRNF144a#2 increased H₂O₂-treated U2OS cell viability (Fig. 6C). We also observed that RNF144a overexpression and knockdown regulated H₂O₂-mediated cell death in HeLa cells (Fig. S6A,B). To determine whether cell death is dependent on persistent activation of ERK, we treated the cells with PD98059, which is known as a MAP kinase inhibitor. We observed that increased cell death due to RNF144a overexpression under oxidative stress was rescued by treatment with PD98059. This suggests that persistent activation of ERK is one of the important causes of cell death following overexpression of RNF144a in response to H₂O₂ (Fig. 6D). Finally, to confirm whether VRK3 is an important factor in RNF144a-dependent cell death, we re-introduced VRK3 into cells overexpressing RNF144a. We observed that increased sensitivity to oxidative stress caused by RNF144a was rescued by overexpression of VRK3 (Fig. 6E). Therefore, VRK3 has a protective role in U2OS cells by suppressing excessive ERK activation (Fig. 6F).

DISCUSSION

It is very important to protect cells from external and internal stresses. External stresses (e.g. UV, DNA damaging agents, pathogens and oxidative stresses) and internal stresses (e.g. DNA replication stress, metabolic stress and oxygen radicals) constantly threaten cell survival (Fulda et al., 2010; Kültz, 2005). As cells continue to survive, they need to overcome these stresses and repair the damage that occurs. If these stresses are not handled well, cells can die through apoptosis or necrosis (Proskuryakov et al., 2003). In addition, if cells continue to divide when replication stress is not resolved, the cells may become cancerous (Benz and Yau, 2008; Morry et al., 2017). Thus, the processes that handle these stresses in cells are closely related to cell survival and many diseases.

Oxidative stress is caused by an imbalance between reactive oxygen species and antioxidants, which can directly damage DNA, proteins and lipids in cells (Kannan and Jain, 2000; Redza-Dutordoir and Averill-Bates, 2016; Ryter et al., 2007). The increase in oxidative stress in cells by internal and external factors is closely related to various disorders, including neurodegenerative diseases, cardiovascular diseases, cancer, digestive diseases and skin disorders (Bhattacharyya et al., 2014; Bickers and Athar, 2006; Bueno and Molkenin, 2002; Cui et al., 2012; Dias et al., 2013; Finkel and Holbrook, 2000; Huang et al., 2016; Kregel and Zhang, 2007; Kruk and Duchnik, 2014; Reuter et al., 2010; Smith et al., 2000). In particular, the overactivation of ERK by oxidative stress is closely linked to many degenerative brain diseases. In the case of Alzheimer's disease, amyloid β deposition activates the ERK pathway, and activated ERK induces the hyperphosphorylation of tau and APP, resulting in facilitation of neurodegeneration (Kirovac et al., 2017). In Parkinson's disease patients, pathogenic α -synuclein and Lewy bodies activate the ERK pathway in microglia and promote the secretion of pro-inflammatory cytokines such as interleukin-1 β and TNF (Klegeris et al., 2008). It has also been reported that activated ERK is found in the Lewy body, which consists of aggregated α -synuclein (Zhu et al., 2002). In many other diseases, sustained ERK activation has been observed as well. ERK activation is very closely associated with cardiac vascular disease (Talmor et al., 2000). ERK signaling pathways have been reported to increase cardiac hypertrophy in MEK1 (also known as MAP2K1) transgenic mice (Bueno et al., 2000). In addition, several studies have shown that ERK activity is increased in ischemia (Friguls et al., 2002). Abnormal ERK activity is closely related to the growth of cancer cells, and inhibition of ERK activity is considered to be an important anticancer strategy (Roberts and Der, 2007). Because

the persistent activation of ERK increases cell death, ERK inhibitors have already been applied to many diseases. PD98059, which inhibits the activity of ERK, has been reported to protect cells from damage caused by brain ischemia (Alessandrini et al., 1999). In glial cells, the ERK inhibitor U0126, in addition to PD98059, reduces neuronal degeneration induced by ERK overactivation (Subramaniam et al., 2004). Furthermore, it has been reported that oral intake of PD90605 delays myocardial remodeling induced by NO synthase inhibition *in vivo* (Sanada et al., 2003). Therefore, tight regulation of ERK signaling is very important for cell survival and the treatment of many diseases.

vVRK3 protects cells via downregulation of ERK activity in stress situations (Kang and Kim, 2006). However, it is not clear how VRK3 is regulated when cells die from strong external stresses. Interestingly, VRK3 protein level gradually decreased over time when cells were under strong stress. Through this, we confirmed that the cyto-protective effect of VRK3 was inhibited by the degradation of VRK3 under persistent and strong stress. It will be interesting to compare the level and localization of VRK3 in mild and intense stress situations. According to our previous report, the level of VRK3 in the SHSY5Y cell line does not change significantly under oxidative stress (Song et al., 2016a). However, it was confirmed that the level of VRK3 is gradually decreased by oxidative stress in U2OS, HeLa and HMO6 cells. Therefore, comparing the degradation rate of VRK3 with the rate of cell death may give us a hint to find a new standard that could determine how each cell responds to oxidative stress. We also observed that the levels of VRK2, but not VRK1, were gradually decreased under oxidative stress. In the future, it will be necessary to figure out why VRK2 is also decreased under oxidative stress and whether RNF144a is involved in this process.

We observed that VRK3 migrates from the nucleus to the cytoplasm in response to oxidative stress. Changes in localization of VRK3 from the nucleus to the cytoplasm increase the chance of interaction with RNF144a, thereby promoting the breakdown of VRK3. However, it is unclear how VRK3 changes its localization from the nucleus to the cytoplasm under oxidative stress. Further studies will be needed to determine whether there is a posttranslational modification of VRK3 that modulates its localization or whether there could be other factors that may help translocation of VRK3. According to previous studies, there are many examples where oxidative stress changes the localization of proteins. For example, SOD1 is known to change localization from cytoplasm to nucleus in response to H₂O₂, and pancreatic transcription factor PDX1 is found to translocate from the nucleus to the cytoplasm upon oxidative stress (Kawamori et al., 2003; Tsang et al., 2014). Therefore, we can hypothesize that there is a specific mechanism to regulate localization of VRK3 under oxidative stress, as shown in the above reports.

RNF144a degrades DNA-PK and increases apoptosis when DNA is damaged (Ho et al., 2014). Therefore, RNF144a appears to increase apoptosis when external stresses such as DNA damage and oxidative stress occur. On the other hand, in EGF signaling, which promotes cell proliferation, RNF144a appears to play the opposite role, which continuously increases cell survival and proliferation (Ho and Lin, 2018). It is known that EGFR is activated by hydrogen peroxide, but when RNF144a was overexpressed, the activity of ERK was still maintained at a level higher than that of controls, even though an EGFR inhibitor was applied. This suggests that there is another means of regulating the ERK signaling pathway in stressful situations (Khan et al., 2006). This shows that RNF144a is an E3 ligase molecule that regulates both cell proliferation and cell death by ubiquitinating its target proteins in various situations.

Taken together, our data demonstrate that VRK3 is translocated from the nucleus to the cytoplasm under oxidative stress, resulting in

increased interaction with RNF144a. Increased polyubiquitylation of VRK3 by RNF144a promoted the degradation of VRK3. VRK3 was originally known to protect cells by preventing excessive and persistent ERK activation, but the degradation of VRK3 by RNF144a makes cells more vulnerable to oxidative stress and eventually increases apoptosis. Because treatment with PD98059 rescued the cell death induced by oxidative stress, this suggests that the regulation of ERK signaling by VRK3 plays an important role in cell survival and death. In conclusion, our findings may contribute to the understanding of the function of cells in various diseases and stressful situations caused by persistent ERK activation.

MATERIALS AND METHODS

Plasmids

The coding regions of *VRK3* and *RNF144a* were amplified by PCR from SHSY5Y and U2OS cells and cloned into PGEX-4T3 (Amersham Biosciences), pFlag-CMV2 (Sigma-Aldrich), PEGFP-C1 (BD Biosciences), pcDNA3.1 (Invitrogen) and pProEX-Hta (Invitrogen) vectors. We used the fragments of VRK3 F1 (amino acids 1–165), F2 (amino acids 166–340) and F3 (amino acids 166–474) that are reported in a previous paper (Song et al., 2016a).

Cell culture, transfection and immunoblotting

HEK293A and HeLa cell lines were obtained from the Korean Cell Line Bank (Korea). U2OS cells were purchased from American Type Culture Collection (USA). HMO6 cells were gifted by Professor S. U. Kim (University of British Columbia, Canada). HEK293A, HeLa, HMO6 and U2OS cells were cultured in Dulbecco's modified Eagle's medium (DMEM) with high glucose (HyClone) containing 10% fetal bovine serum (FBS; HyClone) and 1% penicillin G and streptomycin (Welgene) in a humidified 5% CO₂ incubator at 37°C. Transient transfection was performed using an MP-100 microporator (Invitrogen) according to the manufacturer's instructions. For immunoblotting, cells were disrupted with cell lysis buffer [20 mM Tris, 150 mM NaCl, 1 mM EDTA, 0.5% Triton-X 100 and protease inhibitors (Roche)], followed by sonication. 20–30 µg of protein samples were loaded for SDS-PAGE and transferred to nitrocellulose membrane. Images were obtained using an LAS-4000 system (Fujifilm).

Chemicals and antibodies

Hydrogen peroxide was purchased from Santa Cruz Biotechnology. MG132 was purchased from Calbiochem. PD98059, Hoechst 33342 and Leptomycin B were purchased from Sigma-Aldrich. Anti-VRK3 (#3260; 1:500), anti-Flag (#2368; 1:1000), anti-phospho-ERK T202/Y204 (#4370; 1:1000), anti-ERK (#4695; 1:1000), anti-His (#2365; 1:1000), anti-GST (#2625; 1:1000), anti-phospho-AKT S473 (#4060; 1:1000), anti-AKT (#2920; 1:1000) and anti-cleaved caspase 3 (#9664; 1:300) antibodies were purchased from Cell Signaling Technology, as was the normal rabbit IgG (#2729). Anti-GAPDH (sc-47724; 1:5000), anti-laminA/C (sc-6215; 1:1000), anti-ubiquitin (sc-8017; 1:1000) and anti-EGFR (sc-03; 1:1000) antibodies were purchased from Santa Cruz Biotechnology. Anti-RNF144a (ab89260; 1:500) and anti-VRK3 (ab220830; 1:1000) antibodies were purchased from Abcam, as was the VeriBlot IP detection reagent (ab131366; 1:200). Anti-HA (A190-108A; 1:1000) antibody was purchased from Bethyl Laboratories. Anti-p-EGFR (44-788G; 1:1000) antibody was purchased from Life Technologies. Anti-RNF144a (orb214931; 1:200) antibody was purchased from Biorbyt. Anti-RNF144a (PA5-36451; 1:200) antibody was purchased from Invitrogen.

Immunofluorescence

U2OS cells were transfected with EGFP-VRK3 and grown on 0.1%-gelatin-coated glass chips in 6-well plates. Transfected cells were fixed in 4% paraformaldehyde for 30 min and washed three times with phosphate-buffered saline (PBS). Cells were permeabilized with 0.5% NP-40 for 30 min and blocked with blocking solution (5% FBS, 2.5% BSA and 0.3%

Triton x-100) for 2 h at room temperature. After permeabilization, cells were incubated with primary antibody overnight at 4°C. Then, the cells were incubated with Alexa Fluor 488- (1:500) and Alexa Fluor 594-conjugated (1:500) secondary antibodies in blocking solution for 2 h. Nuclei of cells were stained with 2 µg/ml of Hoechst 33342 for 10 min. Images were obtained using a laser scanning confocal microscope (model FV3000; Olympus) and a Zeiss fluorescence microscope. Image analysis was performed using the FV31S-SW Fluoviewer software (Olympus).

Purification of recombinant protein

All GST-tagged recombinant proteins were expressed in *E. coli* BL21-Codon Plus (DE3) RIPL strain (Agilent Technologies). Transformed *E. coli* were grown at 37°C in LB medium until an OD₆₀₀ of 0.6–0.8 was reached before 0.5 M IPTG was added for protein expression induction. After protein induction at 18°C for 24 h, *E. coli* were resuspended with cold PBS, and the cells disrupted using sonication. Recombinant proteins were purified using Glutathione Sepharose 4B beads (GE Healthcare Bio-Sciences). All His-tagged recombinant proteins were purified using the same protocol as for the GST-tagged recombinant proteins, except using Ni-NTA agarose beads (Invitrogen) instead of Glutathione Sepharose 4B beads.

GST pulldown assay

GST or GST-tagged recombinant proteins were mixed with His-tagged recombinant proteins in cell lysis buffer (20 mM Tris, 150 mM NaCl, 1 mM EDTA and 0.5% Triton-X) and the mixture was incubated overnight at 4°C on a rotator. After incubation, Glutathione Sepharose 4B beads were washed three times with cold lysis buffer. After washing, 20 µl of 2× sample buffer and 1 mM DTT were added, and the sample was heated at 95°C for 7 min. The mixture was analyzed by immunoblotting.

Immunoprecipitation

HEK293A cells were resuspended in cell lysis buffer and disrupted using sonication. 1 mg of HEK293A cell lysate was incubated with protein A-agarose beads (Roche) and each antibody overnight at 4°C on a rotator. After incubation, beads were washed three times with cold lysis buffer. 20 µl of 2× sample buffer and 1 mM DTT were added to the mixture, and the sample was heated at 95°C for 7 min. The mixture was analyzed by immunoblotting.

Fractionation of cytosol and nucleus

To prepare cytoplasmic extracts, U2OS cells were lysed in cytoplasmic extraction buffer (10 mM HEPES pH 7.4, 10 mM KCl and 0.05% NP-40) on ice for 20 min. After incubation, cell lysates were centrifuged at 848 g for 10 min and the supernatant was collected. To prepare nuclear extracts, the pellets were resuspended in cell lysis buffer (20 mM Tris, 150 mM NaCl, 1 mM EDTA and 0.5% Triton-X) and sonicated.

Ubiquitylation assay

HEK293A cells were transfected with vectors, and cells were treated with 10 µM MG132 for 4 h. Cell lysates were prepared in cell lysis buffer [20 mM Tris, 150 mM NaCl, 1 mM EDTA, 0.5% Triton-X and protease inhibitors (Roche)] and disrupted using sonication. Cell lysates were incubated overnight at 4°C with anti-Flag antibody and protein A-agarose beads (Roche). After incubation, beads were washed three times with cell lysis buffer and 10 mM DTT and 2× sample buffer were added to the beads. The mixture was heated at 95°C for 7 min and analyzed by immunoblotting.

Cell viability assay

U2OS cells were subcultured in 96-well plates at a density of 1×10⁴ cells per well. Cells were treated at the indicated times with indicated reagents (hydrogen peroxide, PD98059). After incubation, cells were treated with the addition of 25 µl of 5 mg/ml 3-(4,5-dimethylthiazol-2-yl)-2,5-diphenyltetrazolium bromide (MTT) to each well and then incubated for a further 2 h. The medium containing MTT was removed, and 100 µl of DMSO was added to each well. The absorbance was measured at 570 nm using an Infinite 200 Pro NanoQuant (TECAN).

RNA isolation and reverse transcription qPCR

U2OS cells were mixed with 700 μ l of Tri-solution (Bio Science Technology), and total RNA was extracted by adding 140 μ l of chloroform. After incubation at room temperature for 10 min, samples were centrifuged at 12,000 *g* at 4°C for 10 min. The upper phase was transferred to a fresh tube and mixed with an equal volume of isopropanol. After 10 min incubation at room temperature, samples were centrifuged again. The white RNA pellet was washed with 75% ethanol and dissolved with DEPC-treated water. Total RNA was reverse transcribed using ImProm-II™ Reverse Transcription System (Promega), following the manufacturer's instructions. qPCR was performed using a StepOnePlus Real-Time PCR System (Applied Biosystems) with FastStart Universal SYBR Green Master (Roche).

Statistical analysis

Statistical analyses were performed using GraphPad Prism version 8.0. Two-tailed unpaired Student's *t*-test, one-way ANOVA and repeated measure ANOVA were used to determine significance. Values of $P < 0.05$, $P < 0.01$, $P < 0.001$ and $P < 0.0001$ are indicated by *, **, *** and ****, respectively. All error bars shown in this study represent standard deviation (s.d.).

Competing interests

The authors declare no competing or financial interests.

Author contributions

Conceptualization: S.H.H., K.-T.K.; Methodology: S.H.H.; Validation: S.H.H., K.-T.K.; Formal analysis: S.H.H.; Investigation: S.H.H., K.-T.K.; Resources: S.H.H., K.-T.K.; Writing - original draft: S.H.H., K.-T.K.; Writing - review & editing: S.H.H., K.-T.K.; Supervision: K.-T.K.; Project administration: S.H.H., K.-T.K.; Funding acquisition: K.-T.K.

Funding

This study was supported by BK21 Plus funded by the Ministry of Education (10220130012243), the Bio & Medical Technology Development Program of the National Research Foundation of Korea (2017M3C7A1023478), the Cooperative Research Program for Agriculture Science and Technology Development of the Rural Development Administration (Project No. PJ01324801), and the Basic Science Research Program through the National Research Foundation of Korea funded by the Ministry of Education (2019R1A2C2009440).

Supplementary information

Supplementary information available online at <https://jcs.biologists.org/lookup/doi/10.1242/jcs.247304.supplemental>

References

- Alessandrini, A., Namura, S., Moskowitz, M. A. and Bonventre, J. V. (1999). MEK1 protein kinase inhibition protects against damage resulting from focal cerebral ischemia. *Proc. Natl. Acad. Sci. USA* **96**, 12866-12869. doi:10.1073/pnas.96.22.12866
- Benz, C. C. and Yau, C. (2008). Ageing, oxidative stress and cancer: paradigms in parallax. *Nat. Rev. Cancer* **8**, 875-879. doi:10.1038/nrc2522
- Bhattacharyya, A., Chattopadhyay, R., Mitra, S. and Crowe, S. E. (2014). Oxidative stress: an essential factor in the pathogenesis of gastrointestinal mucosal diseases. *Physiol. Rev.* **94**, 329-354. doi:10.1152/physrev.00040.2012
- Bickers, D. R. and Athar, M. (2006). Oxidative stress in the pathogenesis of skin disease. *J. Invest. Dermatol.* **126**, 2565-2575. doi:10.1038/sj.jid.5700340
- Bueno, O. F. and Molkentin, J. D. (2002). Involvement of extracellular signal-regulated kinases 1/2 in cardiac hypertrophy and cell death. *Circ. Res.* **91**, 776-781. doi:10.1161/01.RES.0000038488.38975.1A
- Bueno, O. F., De Windt, L. J., Tymitz, K. M., Witt, S. A., Kimball, T. R., Klevitsky, R., Hewett, T. E., Jones, S. P., Lefer, D. J., Peng, C. F. et al. (2000). The MEK1-ERK1/2 signaling pathway promotes compensated cardiac hypertrophy in transgenic mice. *EMBO J.* **19**, 6341-6350. doi:10.1093/emboj/19.23.6341
- Cagnol, S. and Chambard, J.-C. (2010). ERK and cell death: mechanisms of ERK-induced cell death—apoptosis, autophagy and senescence. *FEBS J.* **277**, 2-21. doi:10.1111/j.1742-4658.2009.07366.x
- Colucci-D'Amato, L., Perrone-Capano, C. and di Porzio, U. (2003). Chronic activation of ERK and neurodegenerative diseases. *BioEssays* **25**, 1085-1095. doi:10.1002/bies.10355
- Cui, H., Kong, Y. and Zhang, H. (2012). Oxidative stress, mitochondrial dysfunction, and aging. *J. Signal. Transduct.* **2012**, 646354. doi:10.1155/2012/646354
- Dias, V., Junn, E. and Mouradian, M. M. (2013). The role of oxidative stress in Parkinson's disease. *J. Parkinsons Dis.* **3**, 461-491. doi:10.3233/JPD-130230
- El-Rayes, B. F. and LoRusso, P. M. (2004). Targeting the epidermal growth factor receptor. *Br. J. Cancer* **91**, 418-424. doi:10.1038/sj.bjc.6601921
- Finkel, T. and Holbrook, N. J. (2000). Oxidants, oxidative stress and the biology of ageing. *Nature* **408**, 239-247. doi:10.1038/35041687
- Friguls, B., Petegnief, V., Justicia, C., Pallàs, M. and Planas, A. M. (2002). Activation of ERK and Akt signaling in focal cerebral ischemia: modulation by TGF- α and involvement of NMDA receptor. *Neurobiol. Dis.* **11**, 443-456. doi:10.1006/nbdi.2002.0553
- Fu, L., Liu, K. K., Sun, M. G., Tian, C. P., Sun, R., Betanzos, C. M., Tallman, K. A., Porter, N. A., Yang, Y., Guo, D. J. et al. (2017). Systematic and quantitative assessment of hydrogen peroxide reactivity with cysteines across human proteomes. *Mol. Cell. Proteomics* **16**, 1815-1828. doi:10.1074/mcp.RA117.000108
- Fulda, S., Gorman, A. M., Hori, O. and Samali, A. (2010). Cellular stress responses: cell survival and cell death. *Int. J. Cell Biol.* **2010**, 214074. doi:10.1155/2010/214074
- Ho, S.-R. and Lin, W.-C. (2018). RNF144A sustains EGFR signaling to promote EGF-dependent cell proliferation. *J. Biol. Chem.* **293**, 16307-16323. doi:10.1074/jbc.RA118.002887
- Ho, S.-R., Mahanic, C. S., Lee, Y.-J. and Lin, W.-C. (2014). RNF144A, an E3 ubiquitin ligase for DNA-PKcs, promotes apoptosis during DNA damage. *Proc. Natl. Acad. Sci. USA* **111**, E2646-E2655. doi:10.1073/pnas.1323107111
- Huang, W.-J., Zhang, X. and Chen, W.-W. (2016). Role of oxidative stress in Alzheimer's disease. *Biomed. Rep.* **4**, 519-522. doi:10.3892/br.2016.630
- Kang, T.-H. and Kim, K.-T. (2006). Negative regulation of ERK activity by VRK3-mediated activation of VHR phosphatase. *Nat. Cell Biol.* **8**, 863-869. doi:10.1038/ncb1447
- Kang, T.-H. and Kim, K.-T. (2008). VRK3-mediated inactivation of ERK signaling in adult and embryonic rodent tissues. *Biochim. Biophys. Acta* **1783**, 49-58. doi:10.1016/j.bbamcr.2007.10.011
- Kang, M.-S., Choi, T.-Y., Ryu, H. G., Lee, D., Lee, S.-H., Choi, S.-Y. and Kim, K.-T. (2017). Autism-like behavior caused by deletion of vaccinia-related kinase 3 is improved by TrkB stimulation. *J. Exp. Med.* **214**, 2947-2966. doi:10.1084/jem.20160974
- Kannan, K. and Jain, S. K. (2000). Oxidative stress and apoptosis. *Pathophysiology* **7**, 153-163. doi:10.1016/S0928-4680(00)00053-5
- Kawamori, D., Kajimoto, Y., Kaneto, H., Umayahara, Y., Fujitani, Y., Miyatsuka, T., Watada, H., Leibiger, I. B., Yamasaki, Y. and Hori, M. (2003). Oxidative stress induces nucleo-cytoplasmic translocation of pancreatic transcription factor PDX-1 through activation of c-Jun NH(2)-terminal kinase. *Diabetes* **52**, 2896-2904. doi:10.2337/diabetes.52.12.2896
- Khan, E. M., Heidinger, J. M., Levy, M., Lisanti, M. P., Ravid, T. and Goldkorn, T. (2006). Epidermal growth factor receptor exposed to oxidative stress undergoes Src- and caveolin-1-dependent perinuclear trafficking. *J. Biol. Chem.* **281**, 14486-14493. doi:10.1074/jbc.M509332200
- Kim, E. K. and Choi, E.-J. (2010). Pathological roles of MAPK signaling pathways in human diseases. *Biochim. Biophys. Acta* **1802**, 396-405. doi:10.1016/j.bbadis.2009.12.009
- Kirouac, L., Rajic, A. J., Cribbs, D. H. and Padmanabhan, J. (2017). Activation of Ras-ERK signaling and GSK-3 by amyloid precursor protein and amyloid beta facilitates neurodegeneration in Alzheimer's disease. *eNeuro* **4**, ENEURO.0149-16. doi:10.1523/ENEURO.0149-16.2017
- Klegeris, A., Pelech, S., Giasson, B. I., Maguire, J., Zhang, H., McGeer, E. G. and McGeer, P. L. (2008). α -synuclein activates stress signaling protein kinases in THP-1 cells and microglia. *Neurobiol. Aging* **29**, 739-752. doi:10.1016/j.neurobiolaging.2006.11.013
- Kondoh, K. and Nishida, E. (2007). Regulation of MAP kinases by MAP kinase phosphatases. *Biochim. Biophys. Acta* **1773**, 1227-1237. doi:10.1016/j.bbamcr.2006.12.002
- Kregel, K. C. and Zhang, H. J. (2007). An integrated view of oxidative stress in aging: basic mechanisms, functional effects, and pathological considerations. *Am. J. Physiol. Regul. Integr. Comp. Physiol.* **292**, R18-R36. doi:10.1152/ajpregu.00327.2006
- Kruk, J. and Duchnik, E. (2014). Oxidative stress and skin diseases: possible role of physical activity. *Asian Pac. J. Cancer Prev.* **15**, 561-568. doi:10.7314/APJCP.2014.15.2.561
- Kültz, D. (2005). Molecular and evolutionary basis of the cellular stress response. *Annu. Rev. Physiol.* **67**, 225-257. doi:10.1146/annurev.physiol.67.040403.103635
- Lake, D., Corrêa, S. A. and Müller, J. (2016). Negative feedback regulation of the ERK1/2 MAPK pathway. *Cell. Mol. Life Sci.* **73**, 4397-4413. doi:10.1007/s00018-016-2297-8
- Lee, Y.-J., Cho, H.-N., Soh, J.-W., Jhon, G. J., Cho, C.-K., Chung, H.-Y., Bae, S., Lee, S.-J. and Lee, Y.-S. (2003). Oxidative stress-induced apoptosis is mediated by ERK1/2 phosphorylation. *Exp. Cell Res.* **291**, 251-266. doi:10.1016/S0014-4827(03)00391-4
- Lu, Z. and Xu, S. (2006). ERK1/2 MAP kinases in cell survival and apoptosis. *IUBMB Life* **58**, 621-631. doi:10.1080/15216540600957438

- Morry, J., Ngamcherdtrakul, W. and Yantasee, W. (2017). Oxidative stress in cancer and fibrosis: opportunity for therapeutic intervention with antioxidant compounds, enzymes, and nanoparticles. *Redox Biol.* **11**, 240-253. doi:10.1016/j.redox.2016.12.011
- Nichols, R. J. and Traktman, P. (2004). Characterization of three paralogous members of the Mammalian vaccinia related kinase family. *J. Biol. Chem.* **279**, 7934-7946. doi:10.1074/jbc.M310813200
- Park, B. G., Yoo, C. I., Kim, H. T., Kwon, C. H. and Kim, Y. K. (2005). Role of mitogen-activated protein kinases in hydrogen peroxide-induced cell death in osteoblastic cells. *Toxicology* **215**, 115-125. doi:10.1016/j.tox.2005.07.003
- Park, C.-H., Ryu, H. G., Kim, S.-H., Lee, D., Song, H. and Kim, K.-T. (2015). Presumed pseudokinase VRK3 functions as a BAF kinase. *Biochim. Biophys. Acta* **1853**, 1738-1748. doi:10.1016/j.bbamcr.2015.04.007
- Pearson, G., Robinson, F., Beers Gibson, T., Xu, B. E., Karandikar, M., Berman, K. and Cobb, M. H. (2001). Mitogen-activated protein (MAP) kinase pathways: regulation and physiological functions. *Endocr. Rev.* **22**, 153-183. doi:10.1210/edrv.22.2.0428
- Perry, G., Roder, H., Nunomura, A., Takeda, A., Friedlich, A. L., Zhu, X., Raina, A. K., Holbrook, N., Siedlak, S. L., Harris, P. L. R. et al. (1999). Activation of neuronal extracellular receptor p53 activity is enhanced by a redox-sensitive TP53INP1 SUMOylation. *Cell Death Differ.* **21**, 1107-1118. doi:10.1038/cdd.2014.28
- Peugeot, S., Bonacci, T., Soubeyran, P., Iovanna, J. and Dusetti, N. J. (2014). Oxidative stress-induced p53 activity is enhanced by a redox-sensitive TP53INP1 SUMOylation. *Cell Death Differ.* **21**, 1107-1118. doi:10.1038/cdd.2014.28
- Proskuryakov, S. Y., Konoplyannikov, A. G. and Gabai, V. L. (2003). Necrosis: a specific form of programmed cell death? *Exp. Cell Res.* **283**, 1-16. doi:10.1016/S0014-4827(02)00027-7
- Redza-Dutordoir, M. and Averill-Bates, D. A. (2016). Activation of apoptosis signalling pathways by reactive oxygen species. *Biochim. Biophys. Acta* **1863**, 2977-2992. doi:10.1016/j.bbamcr.2016.09.012
- Reuter, S., Gupta, S. C., Chaturvedi, M. M. and Aggarwal, B. B. (2010). Oxidative stress, inflammation, and cancer: how are they linked? *Free Radic. Biol. Med.* **49**, 1603-1616. doi:10.1016/j.freeradbiomed.2010.09.006
- Roberts, P. J. and Der, C. J. (2007). Targeting the Raf-MEK-ERK mitogen-activated protein kinase cascade for the treatment of cancer. *Oncogene* **26**, 3291-3310. doi:10.1038/sj.onc.1210422
- Ryter, S. W., Kim, H. P., Hoetzel, A., Park, J. W., Nakahira, K., Wang, X. and Choi, A. M. K. (2007). Mechanisms of cell death in oxidative stress. *Antioxid Redox Signal.* **9**, 49-89. doi:10.1089/ars.2007.9.49
- Sacks, D. B. (2006). The role of scaffold proteins in MEK/ERK signalling. *Biochem. Soc. Trans.* **34**, 833-836. doi:10.1042/BST0340833
- Sanada, S., Node, K., Minamino, T., Takashima, S., Ogai, A., Asanuma, H., Ogita, H., Liao, Y., Asakura, M., Kim, J. et al. (2003). Long-acting Ca²⁺ blockers prevent myocardial remodeling induced by chronic NO inhibition in rats. *Hypertension* **41**, 963-967. doi:10.1161/01.HYP.0000062881.36813.7A
- Scheeff, E. D., Eswaran, J., Bunkoczi, G., Knapp, S. and Manning, G. (2009). Structure of the pseudokinase VRK3 reveals a degraded catalytic site, a highly conserved kinase fold, and a putative regulatory binding site. *Structure* **17**, 128-138. doi:10.1016/j.str.2008.10.018
- Smit, J. J. and Sixma, T. K. (2014). RBR E3-ligases at work. *EMBO Rep.* **15**, 142-154. doi:10.1002/embr.201338166
- Smith, M. A., Rottkamp, C. A., Nunomura, A., Raina, A. K. and Perry, G. (2000). Oxidative stress in Alzheimer's disease. *Biochim. Biophys. Acta* **1502**, 139-144. doi:10.1016/S0925-4439(00)00040-5
- Song, H., Kim, W., Choi, J.-H., Kim, S.-H., Lee, D., Park, C.-H., Kim, S., Kim, D.-Y. and Kim, K.-T. (2016a). Stress-induced nuclear translocation of CDK5 suppresses neuronal death by downregulating ERK activation via VRK3 phosphorylation. *Sci. Rep.* **6**, 28634. doi:10.1038/srep28634
- Song, H., Kim, W., Kim, S.-H. and Kim, K.-T. (2016b). VRK3-mediated nuclear localization of HSP70 prevents glutamate excitotoxicity-induced apoptosis and A β accumulation via enhancement of ERK phosphatase VHR activity. *Sci. Rep.* **6**, 38452. doi:10.1038/srep38452
- Spratt, D. E., Walden, H. and Shaw, G. S. (2014). RBR E3 ubiquitin ligases: new structures, new insights, new questions. *Biochem. J.* **458**, 421-437. doi:10.1042/BJ20140006
- Subramaniam, S., Zirrgiebel, U., von Bohlen Und Halbach, O., Strelau, J., Laliberté, C., Kaplan, D. R. and Unsicker, K. (2004). ERK activation promotes neuronal degeneration predominantly through plasma membrane damage and independently of caspase-3. *J. Cell Biol.* **165**, 357-369. doi:10.1083/jcb.200403028
- Talmor, D., Applebaum, A., Rudich, A., Shapira, Y. and Tirosh, A. (2000). Activation of mitogen-activated protein kinases in human heart during cardiopulmonary bypass. *Circ. Res.* **86**, 1004-1007. doi:10.1161/01.RES.86.9.1004
- Tsang, C. K., Liu, Y., Thomas, J., Zhang, Y. and Zheng, X. F. S. (2014). Superoxide dismutase 1 acts as a nuclear transcription factor to regulate oxidative stress resistance. *Nat. Commun.* **5**, 3446. doi:10.1038/ncomms4446
- Xu, B., Wang, W. X., Guo, H. Y., Sun, Z. L., Wei, Z., Zhang, X. Y., Liu, Z. J., Tischfield, J. A., Gong, Y. Q. and Shao, C. S. (2014). Oxidative stress preferentially induces a subtype of micronuclei and mediates the genomic instability caused by p53 dysfunction. *Mutat. Res. Fund. Mol. Mech. Mutagen.* **770**, 1-8. doi:10.1016/j.mrfmmm.2014.08.004
- Zhang, W. and Liu, H. T. (2002). MAPK signal pathways in the regulation of cell proliferation in mammalian cells. *Cell Res.* **12**, 9-18. doi:10.1038/sj.cr.7290105
- Zhang, Y., Liao, X.-H., Xie, H.-Y., Shao, Z.-M. and Li, D.-Q. (2017). RBR-type E3 ubiquitin ligase RNF144A targets PARP1 for ubiquitin-dependent degradation and regulates PARP inhibitor sensitivity in breast cancer cells. *Oncotarget* **8**, 94505-94518. doi:10.18632/oncotarget.21784
- Zhu, J.-H., Kulich, S. M., Oury, T. D. and Chu, C. T. (2002). Cytoplasmic aggregates of phosphorylated extracellular signal-regulated protein kinases in Lewy body diseases. *Am. J. Pathol.* **161**, 2087-2098. doi:10.1016/S0002-9440(10)64487-2